Carbapenem heteroresistance of KPC-producing *Klebsiella pneumoniae* results from tolerance, persistence and resistance.

[1,2,3,4]Adriana Chiarelli, [1,2,4]Nicolas Cabanel, [1,2,4]Isabelle Rosinski-Chupin, [4,5,6]Thomas Obadia, [7]Raymond Ruimy, [1,9]Thierry Naas, [1,9]Rémy A. Bonnin, [1,2,4]Philippe Glaser*

[1]Evolution and Ecology of Antibiotic Resistance Unit, Institut Pasteur-APHP-University Paris-Saclay. [2]CNRS UMR6047, 75015, Paris, France. [3]Sorbonne Université, Paris, France. [4]Université Paris Cité, Paris, France. [5]Institut Pasteur, Infectious Disease Epidemiology and Analytics G5 Unit, F-75015, Paris, France. [6]Institut Pasteur, Bioinformatics and Biostatistics Hub, F-75015, Paris, France. [7]Department of Bacteriology, Nice Academic Hospital, Nice, France. [8]Université Côte d'Azur, and Inserm, C3M, Nice, France Nice, France. [9]UMR1184 Team RESIST, Faculty of Medicine University Paris-Sud, University Paris-Saclay, French National Reference Center for Antibiotic Resistance: Carbapenemase producing Enterobacteriaceae, Le Kremlin-Bicêtre, France.

* Corresponding author: Philippe GLASER,
Institut Pasteur, 28 Rue du Dr Roux, 75724 Paris Cedex 15, Tel + 33 1 45 68 89 96 –
E-mail: pglaser@pasteur.fr

Running title: Carbapenem heteroresistance of KPC-producing Klebsiella pneumoniae

ABSTRACT

Carbapenemase-producing *Klebsiella pneumoniae* (CPKp) have disseminated globally and represent a major threat in hospitals with few therapeutic options and high mortality rates. Isolates producing the carbapenemase KPC (KPC-Kp) might be classified as susceptible according to clinical breakpoints by antibiotic susceptibility testing (AST), allowing the use of imipenem or meropenem for treatment of infections. However, some KPC-Kp show heteroresistance (HR) to carbapenems, with colonies growing in the inhibition halo of agar-based AST. HR KPC-Kp have been associated with a higher risk of treatment failure. Here, we characterized the diversity of mechanisms behind HR to imipenem of these isolates. By analyzing a diverse collection of CPKp, we showed that HR is frequent among KPC-Kp. By monitoring single HR colony appearance using the ScanLag setup, we discriminated surviving cells in two subpopulations leading to a Gaussian-like distribution of early-appearing colonies, with a delayed emergence compared to colonies arising in the absence of antibiotics, and a long tail of late-appearing colonies. A subset of colonies showed a reduced growth rate. Characterization of surviving populations by AST and whole-genome sequencing of 333 colonies revealed a majority of parental genotypes and a broad landscape of genetic alterations in 28% of the colonies, including gene loss, DNA amplification and point mutations. This unveils the complexity of imipenem HR among KPC-Kp isolates, which involves tolerant and persistent cells, but also resistant bacteria. These observations contribute to a better understanding of reasons behind carbapenem treatment failure of KPC-Kp isolates.

50 **IMPORTANCE**

51 The ability of a bacterium to defeat antibiotics not only depends upon resistance, but also on
52 tolerance and persistence, which allow a bacterial population to temporarily survive high drug
53 doses. Carbapenems are antibiotics of last resort and *Klebsiella pneumoniae* isolates producing
54 the carbapenemase KPC are a threat to hospitals, although they might remain susceptible to
55 carbapenems. However, seemingly homogeneous populations of KPC-*K. pneumoniae* isolates
56 frequently show varying degrees of susceptibility to carbapenem, i.e., a phenomenon called
57 heteroresistance. We characterized bacteria surviving a high dose of imipenem, progressively
58 degraded by the released carbapenemase, by monitoring the growth of the resulting colonies
59 using the ScanLag system, their genome sequence and carbapenem susceptibility. We show
60 that the observed phenotypic diversity combines tolerance, persistence and resistance making
61 the treatment with high doses of carbapenems frequently inefficient.

62 **INTRODUCTION**

63 Antibiotic resistance represents a global health concern. Several bacterial pathogens evolved
64 multi-drug resistance (MDR), critically affecting their clinical management. Carbapenem-
65 resistant Enterobacterales (CRE), including *Klebsiella pneumoniae*, were listed by the World
66 Health Organization as critical priority pathogens for which there is an urgent need to develop
67 new antibiotics (1). Carbapenem resistance may arise from the production of an extended-
68 spectrum ß-lactamase (ESBL) or a cephalosporinase associated with decreased permeability
69 due to mutations in porin genes and/or upregulation of efflux pumps, or resulting from the
70 production of specific carbapenem-hydrolysing β-lactamases (carbapenemases) (2).
71 Carbapenemase-producing *K. pneumoniae* (CPKp) is one of the most feared nosocomial
72 pathogen worldwide (3). Carbapenemases belong to Ambler class A (KPC-type), class B
73 (metallo-β-lactamases IMP, VIM- and NDM-types) or class D (OXA-48-like enzymes) of ß-
74 lactamases (4) with variable occurrence according to geographical areas (5, 6). In clinical
75 practice, CPKp may be treated with high doses of carbapenem depending on the minimum
76 inhibitory concentration (MIC) (7). Indeed, production of a carbapenemase leads to a decreased
77 susceptibility to carbapenems but can remain under clinical breakpoints. However, treatment
78 effectiveness is extremely dependent on the accurate measurement of carbapenem MIC (8), and
79 MIC determination is often challenged by variable resistance levels shown by CPKp, especially
80 those producing the class A carbapenemase KPC (KPC-Kp) (9, 10).

81 A further challenge is represented by heteroresistance (HR) towards carbapenems. Antibiotic
82 HR broadly describes heterogeneous susceptibility levels to an antibiotic within seemingly
83 isogenic bacterial populations. This "bet-hedging" survival strategy confers long-term fitness
84 benefit to populations in constantly fluctuating environments (11). In addition, as resistance is
85 often a stepwise evolutionary process, such heterogeneity may precede genetic changes, and
86 accelerate resistance development in the population (12, 13). Antibiotic HR itself corresponds
87 to different situations according to the clonality of resistant subpopulations compared to the
88 bulk of the population, the resistance level and the stability of the observed phenotype (14).
89 Most of the studies addressing the HR issue adopt the Population Analysis Profiling (PAP)
90 method, although following different parameters. Yet, there is a general consensus that a strain
91 can be defined as HR when showing subpopulations growing at more than eight times the MIC
92 of the main cell population (14).

93 Antibiotic HR has been largely reported among *K. pneumoniae* isolates towards colistin and
94 corresponding to resistant subpopulation due to mutations modifying the LPS charge (15, 16).
95 Although to a minor extent, HR has also been described towards carbapenems (17-20).

96 Carbapenems HR was mostly observed among KPC-Kp (19-21). However, mechanisms
97 mediating carbapenem HR in *K. pneumoniae* remain poorly characterized. Heteroresistant
98 KPC-Kp strains survival upon exposure to high bactericidal concentrations of imipenem (IMP)
99 was shown to result from the emergence of a resistant mutated subpopulations with decreased
100 expression of the major outer membrane porin (OMP), OmpK36 (21, 22). Survival is likely
101 favored in the first place by IMP degradation driven by KPC released into the culture medium,
102 reminding of the phenomenon of indirect resistance, where an antibiotic resistant bacteria
103 contribute to the growth of susceptible ones (23).
104 Here, we aimed at characterizing carbapenem HR in KPC-Kp clinical isolates and identifying
105 metabolic and regulatory pathways underlying the diversity of susceptibility levels to high
106 doses of carbapenems. We characterized phenotypically and genotypically a collection of 62
107 KPC-Kp isolates, in addition to 20 *K. pneumoniae* isolates producing other carbapenemases. A
108 subset of KPC-Kp isolates was further selected to infer the dynamics of bacterial response to
109 high doses of IMP at single colony level (24). Through the characterization of surviving
110 subpopulations, we showed that HR to imipenem in KPC-Kp is a multifaceted phenomenon,
111 which encompasses different mechanisms adopted by bacterial populations to survive drug
112 exposure, namely tolerance, persistence and resistance. This approach also revealed a broad
113 diversity of genetic alterations in diverse pathways associated with the observed phenotypes.
114
115
116 **RESULTS**
117
118 **Diversity of carbapenem resistance and prevalence of heteroresistance among KPC-Kp.**
119 In order to characterize HR among KPC-Kp, we collected 62 KPC-Kp clinical isolates. For
120 comparison, we included 20 clinical isolates expressing other carbapenemases and three clinical
121 isolates without any carbapenemase as control (Table S1). Whole genome sequence (WGS)
122 analysis revealed that the KPC-Kp isolates belong to 16 STs, with ST512 being the most
123 prevalent (n = 19), followed by ST101 (n = 10) and ST258 (n = 8). Thirteen different capsular
124 types were identified, with KL107 being the most represented one (n = 24) and mostly
125 associated with ST512. In addition to the carbapenemase genes, the 82 CPKp isolates displayed
126 diverse antibiotic resistance genes and porin mutations (Table S1). Defects in at least one of the
127 major porin genes (*ompK35* and *ompK36*) were detected in 66% of isolates (n = 54/82) and,
128 among them, 33% (n = 18/54) co-harbored an ESBL gene. In agreement with previous studies,

129 CPKp ST512 isolates shared a truncated *ompK35* sequence and a G134D135 duplication in the
130 sequence of the OmpK36 L3-loop, resulting in a narrower pore and yielding similar resistance
131 levels as a porin inactivation (25). Likewise, CPKp ST258 isolates exhibited a truncated
132 *ompK35* sequence and, two of them had the same *ompK36* GD duplication. The ten ST101
133 CPKp isolates shared a frameshift mutation in *ompK35* and nine of them also had a TD or GD
134 duplication in *ompK36* and one a D duplication in OmpK36 L3-loop (Table S1).
135 The susceptibility levels to IMP and MEM were determined by Etest strip, as the broth
136 microdilution method might be affected by carbapenem degradation (26). The carbapenemase-
137 producing isolates exhibited a broad range of MICs, from 0.125 to >32 mg/L to MEM and 0.25
138 to >32 mg/L to IMP respectively (Table S1). All the IMP R isolates (n = 19) exhibited defects
139 in the sequence of at least one major porin, with 95% (n=18/19) showing altered sequences of
140 both *ompK35* and *ompK36*. All MEM R isolates (n = 38) but one showed at least one mutation
141 in *ompK35*, with 89% having both *omp* genes disrupted (n = 34). A minority of MEM R isolates
142 (9/38) and IMP R isolates (5/19) carried at least one ESBL gene. This observation suggested
143 that higher carbapenem MICs did not result of the expression of an ESBL in the KPC-Kp
144 isolates we have analyzed but mainly of reduced OM permeability.
145 We next evaluated HR of these isolates based on the appearance of colonies within the
146 inhibition halo induced by the Etest antibiotic gradient strip (Fig. 1A). Isolates showing full
147 contact with the Etest gradient strip (IMP, n = 3; MEM, n = 31) for which HR could not be
148 detected were excluded from the analysis (Fig. 1A). According to the criteria defined in the
149 Methods section, 73% (n = 43/59) and 51% (n = 17/31) of the KPC-Kp isolates were identified
150 by Etest as HR or moderate HR to IMP and MEM, respectively (Fig. 1B, Table S1). A higher
151 rate of IMP HR was detected for isolates otherwise classified as susceptible (78%) or
152 intermediate (80%) based on their MIC compared to resistant ones (67%). In the case of MEM,
153 HR was more frequent with isolates classified as intermediate (58%) (Fig. 1B). In addition,
154 71% of isolates carrying bla_{KPC-2} showed MEM HR isolates, in contrast with only 30% of those
155 harboring bla_{KPC-3} (Fig. 1C). Using the same criteria, HR was also detected by Etest among
156 NDM-producing *K. pneumoniae* (n = 3/5 HR to IMP 2/5 HR to MEM), but was not observed
157 among the VIM- and OXA- and control isolates (Table S1).
158 Altogether, these results showed that our set of isolates harboring bla_{KPC} exhibited a broad
159 range of resistance and HR levels.
160
161 **KPC-Kp isolates show subpopulations growing at high imipenem doses.**

162 Based on MIC values and HR data, we selected seven KPC-Kp in our set of isolates to
163 characterize their response to IMP concentrations 4-, 8- and 10-fold their MICs, as determined
164 by Etest. For comparison, two NDM-Kp, two OXA-Kp and two VIM-Kp were also analyzed
165 (in bold in Table S1). To evaluate the impact of the growth phase on the survival of
166 subpopulations to IMP, bacterial cultures in exponential (EP) and stationary phase (SP) were
167 tested.
168 According to the definition of HR, isolates showing colonies at least at IMP 8xMIC were
169 considered as heteroresistant. We detected HR, to varying degrees, in four KPC-Kp isolates:
170 CNR146C9, CNR121E10, KP H15-21-6 and BIC-1 (Fig. 2A). The highest frequency of
171 survival at 8- and 10-fold MIC of IMP was observed for CNR121E10, followed by CNR146C9,
172 thus confirming their HR profile displayed by Etest. Interestingly, KP H15-21-6 was not HR
173 by Etest, but showed surviving subpopulations by PAP. On the other hand, although NDM
174 isolates showed a HR-like pattern by Etest, they did not show HR by PAP assay at 8-fold MIC
175 of IMP. VIM- and OXA-isolates showed scarce or none ability to grow at 8-fold MIC IMP, in
176 agreement with undetected HR profiles by Etest. Significant differences between EP and SP
177 inoculum were observed for four out of the 13 isolates at 8-fold MIC (Fig. 2B). The two KPC-
178 Kp (CNR146C9 and CNR121E10) and the VIM-Kp (CNR206A5) isolates showed a higher
179 frequency of surviving subpopulations in SP, suggesting a persister-like subpopulation.
180 However, the KP1 strain, producing VIM-1, displayed a higher number of surviving CFUs in
181 EP than in SP. These observations suggested a strain-specific ability to cope differently with
182 high doses of IMP, according to the physiological state of the bacterial population.
183
184 **Subpopulation growth dynamics**.
185 Differences in colony size were noticed on medium supplemented with 8-fold MIC IMP for
186 CNR146C9, CNR121E10, Kp H15-21-6 and BIC-1 (Fig. S1A), indicating an heterogeneous
187 growth of surviving subpopulations in the presence of IMP. To better characterize the dynamics
188 by which subpopulations survive exposure to high IMP concentrations, we tracked appearance
189 and growth of individual colonies in the presence of IMP by ScanLag (24). For comparison, we
190 included in our analysis two KPC-Kp isolates showing scarce or none HR (CNR149B2 and
191 CNR152H4). For these two isolates, colony behavior was investigated at 4xMIC IMP, as the
192 number of CFUs at 8xMIC was below our detection threshold (less or equal than 10^2 CFU/ml).
193 Imipenem MICs for the six selected KPC-Kp isolates ranged from 0.25 to 1.5 mg/L (Table S1).
194 By using ScanLag, we quantified the distribution of colony time of appearance (ToA) of the six
195 isolates over 48 hours onto drug-free and IMP-containing media (Fig. 3A). In the absence of

196 IMP, we observed a narrow normal distribution of ToA for all the isolates, with mean values
197 ranging from 426 to 518 minutes (Table S2, Fig. 3A; cyan blue bars). By contrast, the
198 distribution of colony ToA onto media supplemented with IMP was heterogeneous with a main
199 peak and a tail of varying length, particularly visible in CNR146C9, CNR152H4 and
200 CNR121E10 (Fig. 3A, red bars).
201 The bimodal distribution suggested for the six strains the existence of two subpopulations: an
202 early appearing N1 population corresponding to the main peak of ToA, and a late-appearing
203 N2 population indicated by the tail. To characterize the observed heterogeneity, we attempted
204 to fit the data to a two-component mixed model using ToA as index. This approach allowed us
205 to quantify the proportions of the N1 and N2 subpopulations across the six isolates and the
206 heterogeneous delay in growth (here referred to as lag time extension, LE) of the N1 population
207 relative to the colonies appearing on drug-free media (Fig. 3B, Table S2). To estimate the
208 influence of the bacterial growth phase on the survival rate and on the frequency of
209 subpopulations N1 and N2, we also tracked the colony ToA upon spreading stationary phase
210 (SP) cultures of the six isolates on the drug-free and IMP-supplemented agar media.
211 N1 subpopulation from isolates CNR149B2, Kp H15-21-6 and BIC-1 grown up to EP showed
212 an earlier appearance (LE <2) in comparison with the other three isolates, with LE ≥ 2 (Fig. 3C,
213 green boxplots). Since SP cultures have been shown to be more tolerant to ß-lactams (27), we
214 expected to observe an extended delay in growth for SP cultures exposed to IMP. However, by
215 quantifying the LE of N1 subpopulations, we could detect a significantly longer delay only for
216 CNR149B2 and Kp H15-21-6 in SP compared to EP (Fig. 3C).
217 As previously proposed (28), colonies that appeared later than three standard deviations away
218 from the mean of the main peak distribution (subpopulation N1) were hypothesized as
219 derivative of persister cells, restoring growth only upon gradual exhaustion of IMP below the
220 MIC. We estimated their frequency for the six isolates after plating on 8-fold MIC IMP (4-fold
221 for strains CNR133C4 and CNR152H4) from exponential or stationary phase cultures. The
222 highest frequency of persisters in exponential phase was observed for CNR146C9, whereas
223 BIC-1 exhibited the lowest frequency (Fig. 3D). We did not detect any significant difference in
224 the proportions of persisters between the EP and SP, except for CNR146C9 (p-value = 0.0038),
225 which surprisingly showed a lower occurrence of persisters in SP, in contrast with the increased
226 survival of SP grown bacteria as observed by PAP (Fig. 3D, Table S2).
227 Overall, we observed heterogeneous growth resumption among the selected isolates when
228 plated on high concentrations of IMP (4-fold MIC or 8-fold MIC), which suggested the co-
229 existence of at least two distinct phenotypes in the surviving populations. Both the growth delay

230 (measured as lag time extension) and the proportion of the subpopulations N1 and N2 were
231 strain-specific, likely linked to differences in the genomic backgrounds of the isolates.
232
233 **Genetic heterogeneity associated with the observed heteroresistance**.
234 Antibiotics HR refers to a phenotypically heterogeneous subpopulation within a seemingly
235 isogenic population. However, increased survival might be also linked to genetic alterations.
236 We selected CNR146C9 for in-depth genetic analysis of the HR populations and to better
237 discriminate the events responsible for enhanced survival. To obtain a high quality reference
238 genome, we determined its whole genome sequence by combining long- and short-read
239 sequencing. CNR146C9 hosts two plasmids carrying $bla_{\text{CTX-M-15}}$ and $bla_{\text{KPC-3}}$ of 237,007 bp and
240 110,489 bp, respectively and a circular 52,608 bp-long extrachromosomal phage, previously
241 reported in *K. pneumoniae* ST307 isolates (29) (Table S3).
242 Based on the ToA and colony growth rates as visualized by ScanLag (Fig. 3A), we classified
243 surviving colonies according to three patterns: A, B and C (Fig. S1B). Patterns A and B emerged
244 before the cut-off for persisters (on average 1382 min) and globally correspond to the
245 subpopulation N1. Pattern A included colonies showing wild-type or near wild-type growth
246 rates, whereas pattern B corresponded to colonies with reduced growth rates, as observed by
247 ScanLag. Pattern C colonies emerged after the cut-off for persisters, showing a wild-type
248 growth rate but delayed and variable ToA. They corresponded to the N2 subpopulation, the tail
249 of the ToA distribution. A total of 333 colonies (167 of pattern A, 30 of pattern B and 136 of
250 pattern C) were submitted right after isolation and 2 hour-growth in LB broth to WGS and IMP
251 and MEM MIC determination by Etest. Ninety-four colonies showed at least one genetic
252 modification, including single-nucleotide variations (SNVs), insertions, deletions of bases,
253 plasmid/phage loss and amplification (Fig. 4A) affecting a broad range of functions (Fig. 4B).
254
255 **Pattern A colonies result from tolerance or resistance to IMP.**
256 For most of the A-type colonies (128/167), we did not detect any genetic change. These colonies
257 exhibited MIC values for MEM and IMP and an HR profile determined by Etest similar to the
258 parental strain CNR146C9, suggesting they have survived in the presence of IMP until it
259 reaches a concentration lower than the MIC. Thirty-nine A-isolates showed genetic alterations
260 (Table S4). Most of them were not associated with a decreased susceptibility to both
261 carbapenems (63%). The most recurrent event was the loss of the 52,608 bp extrachromosomal
262 phage (n=12). One ICE and part of the *tra* region from the CTX-M-15 plasmid (n=3) were also
263 lost. Point mutations were also detected among those colonies and affecting different functions

264 like a nonsense mutation in *lysS* encoding one of the two tRNA synthase gene or a mutation in
265 *rpsC* encoding the ribosomal protein S3. Some of these diverse genetic events might have been
266 selected and contributed to longer IMP survival. On the other hand, 15 colonies showed a
267 decreased susceptibility to IMP and MEM ranging from 1.5 mg/L to >32 mg/L. Strikingly, all
268 mutations detected in these colonies except one were associated with alterations of the cell
269 envelope. Mutations leading to the highest MICs affected the OM permeability, with three
270 clones mutated in *ompK36*. However, non-canonical mutations affecting the Bam pathway of
271 insertion of OMP into the outer membrane OM (30) were also selected. Three clones showed a
272 truncated *bamB* gene, one was mutated in *bamA* (N448Y), which is essential, and one isolate
273 showed an IS*Kpn25* insertion six bp upstream of the start codon of the *surA* gene encoding the
274 major chaperon molecule contributing to the translocation of OMP across the periplasm (31).
275 In addition, three clones show mutations affecting LPS biosynthesis and three others mutations
276 in regulatory systems affecting cell wall components. Among these last isolates, AC90-A
277 carried two mutations in the *cpxAR* locus encoding a two component regulatory system sensing
278 OM stresses (32, 33): a four codons deletion (pos. 20 to 23) in the sensor *cpxA*, present in 100%
279 of the reads and a R205W mutation in *cpxR* present in 95% of the reads. This clone is
280 heterogeneous with dominant large colonies, mutated in *cpxR* and *cpxA* showing WT MICs to
281 IMP and MEM and few highly resistant small colonies, only mutated in *cpxA* (Table S4). The
282 only mutation associated with reduced susceptibility but not affecting the cell envelope
283 occurred in the *lipA* gene, involved in lipoyl cofactor biosynthesis. Lipoyl is a cofactor of
284 pyruvate and 2-ketoglutarate dehydrogenases, key enzymes of glycolysis and the tricarboxylic
285 acid (TCA) cycle. This metabolic mutation reminds the type of mutations from the B pattern
286 (see below).
287 Heteroresistance has been shown to result frequently from gene amplification leading to an
288 increased gene expression (34). We systematically searched for DNA amplifications in the 333
289 genomes. We identified three cases of genome amplification among the A-type isolates (Table
290 S4). In strain AC376, we observed a 89,584 bp ectopic duplication encompassing the *dcw* locus
291 encoding major functions for cell wall synthesis and cell division, the additional copy being
292 inserted upstream the transcriptional regulatory gene *qseB* (Fig. 5A). Interestingly, this isolate
293 showed a 16-fold decreased IMP susceptibility but almost no effect on MEM susceptibility.
294 Strain AC150-A showed a c.a. 68 kb-long duplication within the pKPC plasmid and
295 encompassing $bla_{\text{KPC-3}}$ (Fig. 5B). This duplication might be responsible for a doubling of the
296 MICs for IMP and MEM of this strain. On the other hand, the gene coverage of pKPC was
297 variable across all isolates with an average normalized coverage ranging from 0.39 to 2.62

298 excluding isolates which have lost pKPC. The 11 isolates with the highest pKPC coverage
299 (ranging from 1.88 to 2.62-folds higher than the average) all belong to the A class. However,
300 except AC150-A, none showed an increased MIC to IMP and MEM as quantified by E-test.
301
302 **Colonies of B-pattern are mainly small colony variants**
303 Twenty-two out of the 30 B-pattern colonies here analyzed showed an increased MIC for both
304 carbapenems. The eight remaining isolates might have been misclassified as pattern B or the
305 phenotype was highly unstable, as after re-isolation they did not phenotypically differentiate
306 from the parental strains (Table S5). We identified mutations in 28/30 isolates (Table S5) and
307 67% occurred in genes with metabolic functions. The most recurrent mutations affected
308 respiration with mutations found in the coenzyme Q synthesis genes *ubiA* (n=2), *ubiB* (n=2),
309 *ubiD* and *ispA* (n=3), in the heme biosynthesic gene *hemA* and in genes involved in the TCA
310 cycle (a deletion encompassing *lpdA* and *aceF*; *icd*, encoding isocitrate dehydrogenase (n=2)
311 and *acnB*, encoding the aconitate hydratase (n=2)). One isolate showed inactivation of the gene
312 *ptsI* from the central phosphotransferase system (PTS), contributing to carbon source import
313 and catabolic regulation in *E. coli* (35). In the presence of oxygen, these mutants showed tiny
314 colonies with fastidious growth, which are features of small colony variant (SCV) (36). Under
315 these conditions, they also showed an increased resistance to IMP and MEM. However, under
316 anaerobiosis, these phenotypic traits were reversed for respiratory and TCA mutants. Therefore
317 the metabolic defect was likely responsible for the phenotype (Table S5). Two mutations
318 affected lipid metabolism: *pgpC* encoding a phosphatidylglycerophosphatase C and *hldE,*
319 encoding a bifunctional kinase/adenylyltransferase involved in the inner core LPS biosynthesis
320 (37). One isolate mutated in *cysB* showed an increased MICs only towards IMP. Interestingly,
321 *cysB* mutation is the major cause of mecillinam resistance in clinical isolates of *E. coli* (38).
322 One isolate (AC171-B) mutated in the $tRNA^{Ser}$(gct) encoding gene showed a moderate decrease
323 in susceptibility to both carbapenems and a strong growth defect, possibly due to altered protein
324 synthesis. Globally, pattern B corresponded to resistant bacteria with mutations in
325 *K. pneumoniae* core resistome and associated with decreased growth rate, as observed by
326 ScanLag.
327
328 **Pattern C colonies likely correspond to persisters.**
329 Unlike colonies from pattern A and B, none of the pattern C colonies showed a significant
330 increase in the MICs to carbapenems and 86% (n=117/136) did not show any detectable genetic
331 modification. Unexpectedly, ten colonies showed an increased susceptibility to the two

332 carbapenems due to the loss of the pKPC plasmid (Table S6). As observed for pattern A
333 colonies, four patterns C colonies showed loss of the phage, whereas one clone (AC158-C) lost
334 an integrated prophage. In one isolate (AC362-C), we observed a 3-fold copy number increase
335 of a 51 kb long region from the pCTX-M plasmid bracketed by two IS*5075* (Fig. S2). This
336 genomic island contains numerous adaptive functions for glycogen biosynthesis, lactose
337 catabolism, the Fe(3+) dicitrate transport system (*fec* locus) and a glutathione transport system
338 (29). Increased expression of these genes might have contributed to the enhanced survival as
339 persistent cell. Two colonies showed intergenic mutations, while one nonsense mutation
340 inactivates the type VI secretion system protein TssG. Whether these mutations contribute to
341 the persistent phenotype remain to be determined.
342 The late appearance of the colonies and the nature of the seldom genetic events observed that
343 are not contributing to ß-lactam resistance are in agreement with colonies resulting from
344 persistent cells. These bacteria escaped the imipenem bactericidal effect until its concentration
345 became lower than CNRR146C9 IMP MIC (0.5 mg/L) or until it is even below the MIC of a
346 strain devoid of $bla_{\text{KPC-3}}$ (0.19 mg/L).
347
348 **DISCUSSION**
349 Although the expression of the KPC carbapenemase confers reduced susceptibility to
350 carbapenems, MICs for imipenem are frequently below the breakpoint for susceptibility (1
351 mg/L, EUCAST), as we have observed in the set of 62 KPC-Kp clinical isolates analyzed in
352 this work. Such MICs are theoretically compatible with the usage of IMP to treat those isolates,
353 but with an increased risk of resistance selection and treatment escape (7). Moreover,
354 occurrence of HR to IMP may further complicate the management of KPC-Kp isolates in
355 clinical practice.
356 In addition to variable MICs, the KPC isolates here analyzed showed different levels of HR
357 towards IMP and MEM. The proportion of isolates showing HR to IMP was higher than those
358 with an HR profile to MEM. These two carbapenems share similar mode of action by targeting
359 mainly PBP2, but also binding to PBP1a PBP1b. In addition, MEM shows a higher affinity to
360 PBP3 (39), explaining differences in the morphological impact of those two carbapenems on
361 *E. coli* cells (40). On the other hand, IMP is a smaller molecule than MEM and shows a rapid
362 influx through the OM (41). More importantly, under laboratory conditions, IMP is less stable
363 than MEM and is spontaneously degraded (41, 42), likely contributing to the higher rate of HR
364 towards IMP comparted to MEM. We observed a higher proportion of HR towards MEM of
365 isolates expressing KPC-2 compared to those expressing KPC-3 (Fig. 1C), which might be

366 linked to a higher stability (longer half-life) of KPC-2 (43) contributing to a extended
367 degradation of MEM in the solid medium.
368
369 HR has been defined as the occurrence of a bacterial subpopulation surviving treatment at 8x
370 the MIC of the drug (14). In our PAP analyses, at this antibiotic concentration, frequency of
371 survival ranged from 5.3 x 10^{-6} to 4.76 x 10^{-4}. This low frequency challenges the harvest of the
372 surviving population, limiting the use of microscopy for single cell analysis on agarose-pad or
373 microfluidics device such as the mother machine (44). Previous studies addressing HR in KPC-
374 Kp were performed in bulk, following addition of IMP at concentrations higher than the MIC
375 leading to the selection of resistant mutants in the porin gene *ompK36* (21, 22). Here, we applied
376 the ScanLag system (24) to analyze the individual fate of surviving bacteria forming colonies
377 on media supplemented with IMP at 8xMIC or 4xMIC. For the six KPC-Kp isolates analyzed,
378 ScanLag revealed a bimodal profile of colony appearance in the presence of IMP: a Gaussian
379 peak, delayed compared to the peak of appearance of the colonies not exposed to IMP, followed
380 by a tail of late appearing colonies. In addition to the delayed time of appearance, some colonies
381 showed a slower growth rate. Compared to other antibiotics, a specific parameter of HR to ß-
382 lactams in ß-lactamase producing bacteria is the degradation of the antibiotic in the medium.
383 The first Gaussian peak of the surviving populations N1 is consistent with what has been
384 defined as tolerant by adjusting lag time (45). Similarly, the late appearing colonies (N2) in the
385 tail of the distribution, emerging under conditions where the antibiotic is gradually degraded
386 would result from persister cells (28, 45). In agreement with these hypotheses, the vast majority
387 of colonies from N1 and N2 populations of strain CNR146C9 reproduced the same
388 susceptibility and HR phenotype as the parental strain. Comparisons of the six clinical isolates
389 showed different profiles and effects of plating EP or SP bacteria (Fig. 3B and 3D), reflecting
390 different levels of tolerance and persistence towards IMP. Such differences in drug survival are
391 likely due to the genomic context, which remains to be fully investigated. As characterized in
392 experimental models of evolution (46, 47), these features might have been selected in synergy
393 with the selection of antibiotic resistance following drug treatments in the host.
394 One limitation of ScanLag is the absence of information on the first generations before the
395 appearance of a visible colony. The observed delay might be related to an extended lag phase
396 or to a transient slow growth phase reducing susceptibility. We speculated that combining
397 genomic and phenotypic analyses of surviving colonies at 8xMIC would provide additional
398 information on surviving populations. Most of the clones from profile A and C (from N1 and
399 N2 populations respectively) showed a phenotype similar to the parental strain and did not

400 exhibit any genetic events, which is in agreement with tolerance and persistence mechanisms,
401 respectively. The frequent loss of pKPC plasmid in ten of the C-isolates was intriguing. Indeed,
402 no plasmid loss was detected among 196 colonies of the parental strain CNR146C9 growing
403 on antibiotic-free medium. The pKPC carries functions contributing to its stability including a
404 *vapBC* family toxin/antitoxin (TA) locus. VapC toxins inhibit translation by an RNAse activity
405 (48). In *E. coli*, the VapBC TA system was previously reported to contribute to increased rate
406 of persistence (49) and a *vapB* mutant was associated with an extension of lag-time and higher
407 drug tolerance in *E. coli* exposed to intermittent high doses of ampicillin (45). We hypothesized
408 that the loss of pKPC might lead to a transient activation of VapC resulting of the instability of
409 VapB and a growth arrest contributing to the persistent state. Therefore, pKPC loss would be
410 under positive selection in the set-up we have used, supporting the hypothesis that C-type
411 colonies arose mainly from persisters. Interestingly, loss of the KPC-plasmid was previously
412 observed in clinical KPC-Kp isolates (50). In this context, the host response or antibiotic
413 treatments might have contributed to a similar selection of persister cells. However, we cannot
414 rule out the possibility that antibiotic stress contributed to plasmid loss. Among the diverse
415 mutations identified not affecting IMP MIC, some might have occurred by chance. However,
416 they might also have been selected as contributing to persistence or to an increased tolerance
417 like mutation in the lysine tRNA synthetase *lysS*.
418 In addition to mutants with similar MICs as the parental strains, we observed an extremely
419 broad range of mutations leading to increased MIC towards IMP, and, in most cases, also to
420 MEM. Resistant colonies could be classified according to their fitness based on their growth
421 rate, as determined by ScanLag (Fig. S1B). Most isolates showing the less affected fitness under
422 the growth condition used (pattern A) were affected in OM permeability, with mutations in the
423 porin gene *ompK36*, but also in the Bam system and in the major chaperon involved in the
424 insertion of OMP in the OM. We also observed collateral effect of such mutations, like a
425 hypermucoid phenotype for the *bamA* mutant or increased mutation rate in the *polB* isolate.
426 Some mutations involving for instance regulatory systems and disrupting LPS biosynthesis
427 likely affected the OM permeability indirectly (51). On the other hand, mutations from the B
428 pattern showed a strong fitness cost and are reminiscent of SCV. SCV have been described in
429 a broad range of species and are frequently associated with a decreased antibiotic susceptibility
430 (36). However, there are only few reports of SCV in *K. pneumoniae*: in a bone and joint
431 infection (52) and associated with colistin HR in biofilm (53). In both cases, the genetic bases
432 for the SCV phenotype were not identified. As reported in other species, most mutations we
433 have characterized affected aerobic respiration (quinone and heme biosynthesis) and the central

434 metabolism (TCA cycle and glycolysis). Interestingly, both the slow growth and the increased
435 MICs were fully or partially reversed in anaerobic conditions (Table S5). The combination of
436 high resistance in the presence of oxygen and normal growth in its absence might contribute to
437 the selection of such mutation during treatment. However, due to their slow growth under
438 laboratory conditions, they might have been overlooked during diagnosis.
439 The increased MICs observed among HR colonies was shown to be frequently unstable and
440 lost following passages in antibiotic-free medium (14). For different bacteria/antibiotic pairs,
441 HR was shown to result mainly from genomic amplification (34), which can revert by
442 homologous recombination between duplications. Here, we identified only four cases of
443 amplification. The duplication of the CTX-M-15 plasmid region carrying fitness functions
444 might have favored bacterial survival and be selected among colonies from the C-pattern
445 (persistent-like). Two amplifications were associated with a decreased susceptibility to IMP. In
446 the strain AC376, we observed a 89,584 bp duplication encompassing the *dcw* locus encoding
447 major functions for cell wall synthesis and cell division. Interestingly, the duplication was not
448 in tandem, but corresponded to an ectopic copy/paste of the region at position 688,936 (Fig. 5).
449 The insertion was located in the *ygiW* - *qseBC* intergenic region within *ygiW* ribosome binding
450 site (RBS). Interestingly, AC376 showed a 16-fold decrease of IMP susceptibility but almost
451 no effect on MEM susceptibility. This observation is in agreement with previous studies
452 showing that amplification of the *ftsQAZ* genes, part of the *dcw* locus, led to decreased
453 susceptibility to mecillinam, an antibiotic targeting exclusively PBP2 (54). Indeed, both IMP
454 and MEM have a high affinity to PBP2, but MEM has also some further affinity to PBP3 (40).
455 In this case, the amplification and the phenotype were stable. Increased copy number of bla_{KPC}
456 was shown to lead to a higher MIC to carbapenems (10). In strain AC150-A, we observed a 68
457 kb duplication within pKPC leading to a modest increase of IMP and MEM MICs (Fig. 5B,
458 Table S4). In addition, the 11 isolates with the highest pKPC coverage belong to pattern A but,
459 except for AC150-A, no change of IMP and MEM MICs was observed. The higher copy
460 number might have enhanced the survival on plates supplemented with IMP but it is predicted
461 to be unstable and likely not detectable in the experimental set-up we used.
462 For mutations leading to a high fitness cost, we observed frequent reversion of the growth defect
463 and the increased MICs. A typical case was strain AC90-A from the A pattern, which showed
464 MICs identical to the parental strain MICs and was mutated in both *cpxA* and in *cpxR*. The *cpxA*
465 mutation would have been first selected, leading to an hyperactivation of CpxR and in turn to
466 an overexpression of *acrB*, *acrD* and *eefB* efflux systems genes and a repression of the porin
467 gene *ompK36* (32). However, the observed decreased susceptibility to carbapenems was

468 associated with a high fitness cost with the rapid accumulation of suppressor mutations. The
469 secondary mutation in *cpxR*, leading to an increased susceptibility compared to the parental
470 strain, suppresses the effect of the cpxA mutation and compensates for the high cost of the
471 primary mutation. This situation correspond to HR resulting of a mutations with a high fitness
472 cost suppressed by a secondary mutation also reverting the effect on antibiotic susceptibility
473 (14).
474
475 **Conclusion**: HR to IMP in KPC-Kp is the result of a combination of different mechanisms to
476 escape bactericidal antibiotics: collective protection effects, tolerance, persistence and
477 resistance. Inter-strain variations leading to different HR frequencies across the clinical isolates
478 here analyzed reflect the different bacterial response to IMP stress and is likely due to genetic
479 differences that remain to be characterized. The analysis of the bacterial response to antibiotics
480 on solid media compared to liquid culture allows to address the diversity of phenotypes and
481 genotypes of surviving bacteria. Although the majority of colonies did not show any genetic
482 change compared to the parental strains, we observed mutations in a very broad range of
483 functions considerably extending our knowledge of *K. pneumoniae* intrinsic ß-lactam
484 resistome. We hypothesize that mutations affecting these functions might also contribute to
485 IMP treatment failure in patients infected by KPC-Kp isolates.
486
487
488 **Materials and METHODS**
489
490 ***Klebsiella pneumoniae* isolates, media and growth conditions.**
491 The isolates analyzed in this work and their main characteristics are listed in Table S1. It
492 includes 62 KPC-Kp clinical isolates and for comparison, 20 clinical isolates expressing other
493 carbapenemases (OXA-48, n=3; VIM-1, n=11; NDM-1, n=3; isolates co-carrying two
494 carbapenemases, n=3) and three isolates not carrying any carbapenemase gene as control.
495 Bacteria were grown in Mueller-Hinton (MH), Tryptic-Soy Broth (TSB) or Lysogeny broth
496 (LB) and on Tryptic-Soy agar (TSA) or LB agar (LBA) plates. Anaerobic growth was
497 performed in an anaerobic chamber (Genbox BioMérieux SA, Marcy/Etoile, France) by
498 following the manufacturer instructions. Antibiotic susceptibility testing (AST) was performed
499 by Etest (BioMérieux) on Mueller-Hinton Agar (MHA) plates inoculated by flood with 2 ml of
500 bacterial culture (10^6 bacteria/ml). Flood inoculation was selected instead of swab streaking to
501 provide a more uniform inoculation. Imipenem and meropenem breakpoints were according to

502 the EUCAST guidelines (https://www.eucast.org/) Susceptible, $\leq$2 mg/L and Resistant, $\geq$ 4
503 mg/l. Etest experiments also allowed a preliminary screening for HR. We referred to HR as the
504 occurrence of at least 5 colonies within the inhibition halo after 16-20 hours of incubation at 37
505 °C. Isolates with 3 or 4 colonies were defined as "moderately HR" and isolates with less than
506 3 colonies in the halo were classified as "non HR". Isolates showing full contact with the Etest
507 gradient strip for which HR could not be detected were excluded from the analysis (Table S1).
508 Plasmid pKPC stability in strain CNR146C9 was determined by quantifying growth of 194
509 independent colonies isolated on LB plates in LB medium supplemented with 0.5 mg/l MEM.
510 Strain AC420-C which have lost pKPC was used as non-growing control.
511
512 **Population Analysis Profiling (PAP).**
513 Heteroresistance was quantified by PAP, following spreading on agar plate of either stationary
514 phase (SP) bacterial cultures (overnight culture, ON) or exponentially growing bacteria (ON
515 culture diluted 1000 times in TSB and incubated at 37°C until OD_{600}~0.3-0.4 was reached).
516 Bacterial cultures were serially diluted in saline buffer and 100 µl of dilution at OD_{600} of 0.01
517 (an estimate of 10^7 bacteria/ml) were spread evenly using the automatic plater EasySpiral
518 (Interscience) on freshly prepared TSA plates containing IMP at 4-fold, 8-fold and 10-fold the
519 MIC of each isolate, as determined by Etest. The plates were incubated at 37 °C, and colonies
520 were counted at 24 hours., The frequency of survival was calculated as the ratio of CFUs on
521 IMP supplemented medium over CFUs on media without IMP. Given the uncertainty in
522 determining CFUs, we arbitrary set a threshold of 10 colonies per plate (10^2 CFU/ml) for
523 significance. Results were calculated from five independent experiments and expressed as the
524 $\log_{10}$ of the frequency.
525
526 **ScanLag assay and data analysis.**
527 ScanLag assays were performed as described previously (24), but adapted to our purposes:
528 approximately 1-3 x 10^6 cells from mid-EP or SP cultures were spread onto TSA plates
529 supplemented with IMP using the EasySpiral plater. Colony tracking was carried out every 20
530 minutes for 48-hours at 37 °C. Time of appearance (ToA) and colony growth rates were
531 estimated by running MATLAB scripts publicly available at
532 https://github.com/iosonofabio/scanlag (55).
533 Colony ToA distributions were analyzed by using the R package *mixtools* (56). We applied a
534 two-component mixture model to the ToA distributions of both untreated populations and those
535 surviving IMP exposure using expectation–maximization (EM) algorithm by the *normalmixEM*

536 function. Briefly, we jointly estimated the vectors of means μ (estimated ToA mean in each
537 component) and standard deviations Σ as well as the mixing weights λ (corresponding to the
538 initial proportion of colonies, expressed in %) to analyze and quantitatively compare
539 subpopulations across the selected isolates. The delay in growth of IMP exposed populations
540 compared to untreated colonies, hereto referred to as Lag time extension (LE), was quantified
541 as the ratio of mean ToA of N1 cells (first appearing population on IMP plates) over the mean
542 ToA of untreated colonies. The "persister" fraction was estimated using thresholds as
543 previously described (28). Briefly, colonies were considered as deriving from persister cells if
544 they appeared later than three standard deviations away from the mean ToA of the N1
545 population (ToA > $\mu_{N1}+3\Sigma_{N1}$). Persister frequency over the whole population was calculated
546 per each isolate; data were then visualized using *ggplot2* (57).
547
548 **Isolation of surviving colonies.**
549 Surviving colonies were selected from IMP-containing plates, re-isolated on media containing
550 the same IMP concentration and, in parallel, on drug free media. The next day, colonies were
551 picked from IMP plates or from plates without IMP - if the colony did not grow on the IMP
552 plate, and incubated in TSB without antibiotic until mid-exponential phase was reached. The
553 cultures were then used for AST by Etest and DNA extraction for genome sequencing.
554
555 **Whole-genome sequencing and analysis.**
556 Genomic DNAs were extracted by using the DNeasy Blood & Tissue Kit (QIAGEN).
557 *K. pneumoniae* genomes were sequenced by using the Illumina HiSeq2500 or NextSeq500
558 platform, with 100- and 75-nucleotides (nt) paired-end reads respectively. Libraries of
559 *K. pneumoniae* clinical isolates were constructed by using the Nextera XT kit (Illumina) and
560 libraries of CNR146C9 clones selected during ScanLag experiments by using NEBNext Ultra
561 II FS DNA Library prep kit, which provide a more even genome coverage (58). Paired-end
562 reads were assembled into contigs with SPAdes 3.9.0 (59). The complete genome sequence of
563 CNR146C9 was determined by using the long-read PacBio technology. Accurate consensus
564 reads obtained from raw reads with pbccs (https://github.com/nlhepler/pbccs) were assembled
565 with Canu (60). The assembly was polished with Circulator (61) and manually corrected by
566 mapping Illumina reads with Breseq 0.33.2 (62). Variants compared to CNR146C9 complete
567 genome sequence were identified by using Breseq (62). Missing regions and recombination
568 events were identified by analysing the "Unassigned missing coverage evidence" and
569 "Unassigned new junction evidence" sections of the Breseq outputs respectively.

570 Polymorphisms were visually verified by using Tablet (63). Genome sequences were annotated
571 with Prokka 1.14.5 (64) and analysed for MLST and ARG content by using Kleborate (65) and
572 Resfinder 4.0.1 (66). Plasmid incompatibility groups were identified by using PlasmidFinder
573 2.1 (67). Copy number variation was estimated by counting the number of reads per gene and
574 comparing with number of Illumina reads of the parental strain CNR146C9 by using the
575 DESSeq2 R Package (68).
576
577 **Statistical analyses**.
578 All statistical tests and graphical representations were performed using R 4.0.3 with R studio
579 1.3.1093 (69). All statistical tests and graphical representations were performed using R v.4.0-
580 3 (69) using packages *ggplot2* (57) and *ggpubr*
581 (https://rpkgs.datanovia.com/ggpubr/index.html). The log10-transformed distributions of
582 survival frequency for exponentially-growing and stationary phases were compared using
583 Student's T-test. A *p-value* below the 5% threshold was deemed significant.
584
585 **Availability of data**.
586 Sequence data for the clinical isolates have been deposited at DDBJ/EMBL/GenBank
587 (Bioproject ERP133503). CNR146C9 WGS was deposited with the following accession
588 numbers: ERS9645073. Biosamples for the Illumina sequence data are listed in Table S1.
589
590 **ACKNOWLEDGEMENTS**
591 This work was supported by grants from the French National Research Agency IBEID (ANR-
592 10-LABX-62-IBEID) and SEQ2DIAG (ANR-20-PAMR-0010). Adriana Chiarelli is part of the
593 Pasteur - Paris University (PPU) International PhD Program, with funding from the Institut
594 Carnot Pasteur Microbes & Santé, and the European Union's Horizon 2020 research and
595 innovation programme under the Marie Sklodowska-Curie grant agreement No 665807.
596 The authors thank Virgile Andreani and Gregory Bath for discussion on HR, Guilhem Royer
597 for critical reading of the manuscript, Laurence Ma from the Institut Pasteur Biomics platform
598 (C2RT, Institut Pasteur, Paris, France, supported by France Génomique, ANR-10-INBS-09-09
599 and IBISA) for her help with Illumina sequencing.
600
601

602 **REFERENCES**

603

604 1. Tacconelli E, Carrara E, Savoldi A, Harbarth S, Mendelson M, Monnet DL, Pulcini C,
605 Kahlmeter G, Kluytmans J, Carmeli Y, Ouellette M, Outterson K, Patel J, Cavaleri M,
606 Cox EM, Houchens CR, Grayson ML, Hansen P, Singh N, Theuretzbacher U, Magrini
607 N. 2018. Discovery, research, and development of new antibiotics: the WHO priority
608 list of antibiotic-resistant bacteria and tuberculosis. Lancet Infect Dis 18:318-327.
609 2. Nordmann P, Dortet L, Poirel L. 2012. Carbapenem resistance in Enterobacteriaceae:
610 here is the storm! Trends Mol Med 18:263-72.
611 3. Munoz-Price LS, Poirel L, Bonomo RA, Schwaber MJ, Daikos GL, Cormican M,
612 Cornaglia G, Garau J, Gniadkowski M, Hayden MK, Kumarasamy K, Livermore DM,
613 Maya JJ, Nordmann P, Patel JB, Paterson DL, Pitout J, Villegas MV, Wang H,
614 Woodford N, Quinn JP. 2013. Clinical epidemiology of the global expansion of
615 *Klebsiella pneumoniae* carbapenemases. Lancet Infect Dis 13:785-96.
616 4. Bush K, Jacoby GA. 2010. Updated functional classification of beta-lactamases.
617 Antimicrob Agents Chemother 54:969-76.
618 5. David S, Reuter S, Harris SR, Glasner C, Feltwell T, Argimon S, Abudahab K, Goater
619 R, Giani T, Errico G, Aspbury M, Sjunnebo S, Feil EJ, Rossolini GM, Aanensen DM,
620 Grundmann H. 2019. Epidemic of carbapenem-resistant *Klebsiella pneumoniae* in
621 Europe is driven by nosocomial spread. Nat Microbiol 4:1919-1929.
622 6. Bonnin RA, Jousset AB, Chiarelli A, Emeraud C, Glaser P, Naas T, Dortet L. 2020.
623 Emergence of New Non-Clonal Group 258 High-Risk Clones among *Klebsiella*
624 *pneumoniae* Carbapenemase-Producing *K. pneumoniae* Isolates, France. Emerg Infect
625 Dis 26:1212-1220.
626 7. Bassetti M, Peghin M. 2020. How to manage KPC infections. Ther Adv Infect Dis
627 7:2049936120912049.
628 8. Kowalska-Krochmal B, Dudek-Wicher R. 2021. The Minimum Inhibitory
629 Concentration of Antibiotics: Methods, Interpretation, Clinical Relevance. Pathogens
630 10.
631 9. Nordmann P, Cuzon G, Naas T. 2009. The real threat of *Klebsiella pneumoniae*
632 carbapenemase-producing bacteria. Lancet Infect Dis 9:228-36.
633 10. Bulman ZP, Krapp F, Pincus NB, Wenzler E, Murphy KR, Qi C, Ozer EA, Hauser AR.
634 2021. Genomic Features Associated with the Degree of Phenotypic Resistance to
635 Carbapenems in Carbapenem-Resistant *Klebsiella pneumoniae*. mSystems 6:e0019421.
636 11. Dewachter L, Fauvart M, Michiels J. 2019. Bacterial Heterogeneity and Antibiotic
637 Survival: Understanding and Combatting Persistence and Heteroresistance. Mol Cell
638 76:255-267.
639 12. Bódi Z, Farkas Z, Nevozhay D, Kalapis D, Lázár V, Csörgő B, Nyerges Á, Szamecz B,
640 Fekete G, Papp B, Araújo H, Oliveira JL, Moura G, Santos MAS, Székely T, Jr., Balázsi
641 G, Pál C. 2017. Phenotypic heterogeneity promotes adaptive evolution. PLoS Biol
642 15:e2000644.
643 13. Band VI, Weiss DS. 2019. Heteroresistance: A cause of unexplained antibiotic
644 treatment failure? PLoS Pathog 15:e1007726.
645 14. Andersson DI, Nicoloff H, Hjort K. 2019. Mechanisms and clinical relevance of
646 bacterial heteroresistance. Nat Rev Microbiol 17:479-496.
647 15. Band VI, Satola SW, Smith RD, Hufnagel DA, Bower C, Conley AB, Rishishwar L,
648 Dale SE, Hardy DJ, Vargas RL, Dumyati G, Kainer MA, Phipps EC, Pierce R, Wilson
649 LE, Sorensen M, Nilsson E, Jordan IK, Burd EM, Farley MM, Jacob JT, Ernst RK,

650 Weiss DS. 2021. Colistin Heteroresistance Is Largely Undetected among Carbapenem-
651 Resistant *Enterobacterales* in the United States. mBio 12.
652 16. Bardet L, Baron S, Leangapichart T, Okdah L, Diene SM, Rolain JM. 2017.
653 Deciphering Heteroresistance to Colistin in a *Klebsiella pneumoniae* Isolate from
654 Marseille, France. Antimicrob Agents Chemother 61.
655 17. Tan K, Nguyen J, Nguyen K, Huse HK, Nieberg PH, Wong-Beringer A. 2020.
656 Prevalence of the carbapenem-heteroresistant phenotype among ESBL-producing
657 *Escherichia coli* and *Klebsiella pneumoniae* clinical isolates. J Antimicrob Chemother
658 75:1506-1512.
659 18. López-Camacho E, Paño-Pardo JR, Sotillo A, Elías-López C, Martínez-Martínez L,
660 Gómez-Gil R, Mingorance J. 2019. Meropenem heteroresistance in clinical isolates of
661 OXA-48-producing *Klebsiella pneumoniae*. Diagn Microbiol Infect Dis 93:162-166.
662 19. Nodari CS, Ribeiro VB, Barth AL. 2015. Imipenem heteroresistance: high prevalence
663 among Enterobacteriaceae *Klebsiella pneumoniae* carbapenemase producers. J Med
664 Microbiol 64:124-126.
665 20. Pournaras S, Kristo I, Vrioni G, Ikonomidis A, Poulou A, Petropoulou D, Tsakris A.
666 2010. Characteristics of meropenem heteroresistance in *Klebsiella pneumoniae*
667 carbapenemase (KPC)-producing clinical isolates of *K. pneumoniae*. J Clin Microbiol
668 48:2601-4.
669 21. Adams-Sapper S, Nolen S, Donzelli GF, Lal M, Chen K, Justo da Silva LH, Moreira
670 BM, Riley LW. 2015. Rapid induction of high-level carbapenem resistance in
671 heteroresistant KPC-producing *Klebsiella pneumoniae*. Antimicrob Agents Chemother
672 59:3281-9.
673 22. Adams-Sapper S, Gayoso A, Riley LW. 2018. Stress-Adaptive Responses Associated
674 with High-Level Carbapenem Resistance in KPC-Producing *Klebsiella pneumoniae*. J
675 Pathog 2018:3028290.
676 23. Nicoloff H, Andersson DI. 2016. Indirect resistance to several classes of antibiotics in
677 cocultures with resistant bacteria expressing antibiotic-modifying or -degrading
678 enzymes. J Antimicrob Chemother 71:100-10.
679 24. Levin-Reisman I, Gefen O, Fridman O, Ronin I, Shwa D, Sheftel H, Balaban NQ. 2010.
680 Automated imaging with ScanLag reveals previously undetectable bacterial growth
681 phenotypes. Nat Methods 7:737-9.
682 25. Fajardo-Lubian A, Ben Zakour NL, Agyekum A, Qi Q, Iredell JR. 2019. Host
683 adaptation and convergent evolution increases antibiotic resistance without loss of
684 virulence in a major human pathogen. PLoS Pathog 15:e1007218.
685 26. Steward CD, Mohammed JM, Swenson JM, Stocker SA, Williams PP, Gaynes RP,
686 McGowan JE, Jr., Tenover FC. 2003. Antimicrobial susceptibility testing of
687 carbapenems: multicenter validity testing and accuracy levels of five antimicrobial test
688 methods for detecting resistance in Enterobacteriaceae and Pseudomonas aeruginosa
689 isolates. J Clin Microbiol 41:351-8.
690 27. Anderl JN, Zahller J, Roe F, Stewart PS. 2003. Role of nutrient limitation and
691 stationary-phase existence in *Klebsiella pneumoniae* biofilm resistance to ampicillin
692 and ciprofloxacin. Antimicrob Agents Chemother 47:1251-6.
693 28. Levin-Reisman I, Balaban NQ. 2016. Quantitative Measurements of Type I and Type
694 II Persisters Using ScanLag. Methods Mol Biol 1333:75-81.
695 29. Villa L, Feudi C, Fortini D, Brisse S, Passet V, Bonura C, Endimiani A, Mammina C,
696 Ocampo AM, Jimenez JN, Doumith M, Woodford N, Hopkins K, Carattoli A. 2017.
697 Diversity, virulence, and antimicrobial resistance of the KPC-producing *Klebsiella*
698 *pneumoniae* ST307 clone. Microb Genom 3:e000110.

699 30. Hagan CL, Silhavy TJ, Kahne D. 2011. β-Barrel membrane protein assembly by the
700 Bam complex. Annu Rev Biochem 80:189-210.
701 31. Denoncin K, Schwalm J, Vertommen D, Silhavy TJ, Collet JF. 2012. Dissecting the
702 Escherichia coli periplasmic chaperone network using differential proteomics.
703 Proteomics 12:1391-401.
704 32. Srinivasan VB, Vaidyanathan V, Mondal A, Rajamohan G. 2012. Role of the two
705 component signal transduction system CpxAR in conferring cefepime and
706 chloramphenicol resistance in *Klebsiella pneumoniae* NTUH-K2044. PLoS One
707 7:e33777.
708 33. Vogt SL, Raivio TL. 2012. Just scratching the surface: an expanding view of the Cpx
709 envelope stress response. FEMS Microbiol Lett 326:2-11.
710 34. Nicoloff H, Hjort K, Levin BR, Andersson DI. 2019. The high prevalence of antibiotic
711 heteroresistance in pathogenic bacteria is mainly caused by gene amplification. Nat
712 Microbiol 4:504-514.
713 35. Gershanovitch VN, Yourovitskaya NV, Komissarova LV, Bolshakova TN, Erlagaeva
714 RS, Bourd GI. 1975. Catabolite repression in *Escherichia coli* K12 mutants defective in
715 glucose transport. Mol Gen Genet 140:81-90.
716 36. Proctor RA, von Eiff C, Kahl BC, Becker K, McNamara P, Herrmann M, Peters G.
717 2006. Small colony variants: a pathogenic form of bacteria that facilitates persistent and
718 recurrent infections. Nat Rev Microbiol 4:295-305.
719 37. Kneidinger B, Marolda C, Graninger M, Zamyatina A, McArthur F, Kosma P, Valvano
720 MA, Messner P. 2002. Biosynthesis pathway of ADP-L-glycero-beta-D-manno-heptose
721 in *Escherichia coli*. J Bacteriol 184:363-9.
722 38. Thulin E, Sundqvist M, Andersson DI. 2015. Amdinocillin (Mecillinam) resistance
723 mutations in clinical isolates and laboratory-selected mutants of *Escherichia coli*.
724 Antimicrob Agents Chemother 59:1718-27.
725 39. Sutaria DS, Moya B, Green KB, Kim TH, Tao X, Jiao Y, Louie A, Drusano GL, Bulitta
726 JB. 2018. First Penicillin-Binding Protein Occupancy Patterns of β-Lactams and β-
727 Lactamase Inhibitors in *Klebsiella pneumoniae*. Antimicrob Agents Chemother 62.
728 40. Sumita Y, Fukasawa M, Okuda T. 1990. Comparison of two carbapenems, SM-7338
729 and imipenem: affinities for penicillin-binding proteins and morphological changes. J
730 Antibiot (Tokyo) 43:314-20.
731 41. Zhanel GG, Wiebe R, Dilay L, Thomson K, Rubinstein E, Hoban DJ, Noreddin AM,
732 Karlowsky JA. 2007. Comparative review of the carbapenems. Drugs 67:1027-52.
733 42. Nickolai DJ, Lammel CJ, Byford BA, Morris JH, Kaplan EB, Hadley WK, Brooks GF.
734 1985. Effects of storage temperature and pH on the stability of eleven beta-lactam
735 antibiotics in MIC trays. J Clin Microbiol 21:366-70.
736 43. Mehta SC, Rice K, Palzkill T. 2015. Natural Variants of the KPC-2 Carbapenemase
737 have Evolved Increased Catalytic Efficiency for Ceftazidime Hydrolysis at the Cost of
738 Enzyme Stability. PLoS Pathog 11:e1004949.
739 44. Wang P, Robert L, Pelletier J, Dang WL, Taddei F, Wright A, Jun S. 2010. Robust
740 growth of Escherichia coli. Curr Biol 20:1099-103.
741 45. Fridman O, Goldberg A, Ronin I, Shoresh N, Balaban NQ. 2014. Optimization of lag
742 time underlies antibiotic tolerance in evolved bacterial populations. Nature 513:418-21.
743 46. Levin-Reisman I, Brauner A, Ronin I, Balaban NQ. 2019. Epistasis between antibiotic
744 tolerance, persistence, and resistance mutations. Proc Natl Acad Sci U S A 116:14734-
745 14739.
746 47. Levin-Reisman I, Ronin I, Gefen O, Braniss I, Shoresh N, Balaban NQ. 2017. Antibiotic
747 tolerance facilitates the evolution of resistance. Science 355:826-830.

748 48. Winther KS, Gerdes K. 2011. Enteric virulence associated protein VapC inhibits
749 translation by cleavage of initiator tRNA. Proc Natl Acad Sci U S A 108:7403-7.
750 49. Gerdes K, Maisonneuve E. 2012. Bacterial persistence and toxin-antitoxin loci. Annu
751 Rev Microbiol 66:103-23.
752 50. Jousset AB, Bonnin RA, Takissian J, Girlich D, Mihaila L, Cabanel N, Dortet L, Glaser
753 P, Naas T. 2020. Concomitant carriage of KPC-producing and non-KPC-producing
754 *Klebsiella pneumoniae* ST512 within a single patient. J Antimicrob Chemother
755 75:2087-2092.
756 51. Davin-Regli A, Guerin-Faublée V, Pagès JM. 2019. Modification of outer membrane
757 permeability and alteration of LPS in veterinary enterotoxigenic *Escherichia coli*. Res
758 Vet Sci 124:321-327.
759 52. Ronde-Oustau C, Lustig S, Dupieux C, Ferry T. 2017. Implant-associated ESBL-
760 *Klebsiella pneumonia* producing small colony variant bone and joint infection in a
761 healthy 40-year-old man. BMJ Case Rep 2017.
762 53. Silva A, Sousa AM, Alves D, Lourenço A, Pereira MO. 2016. Heteroresistance to
763 colistin in *Klebsiella pneumoniae* is triggered by small colony variants sub-populations
764 within biofilms. Pathog Dis 74.
765 54. Vinella D, Cashel M, D'Ari R. 2000. Selected amplification of the cell division genes
766 *ftsQ-ftsA-ftsZ* in *Escherichia coli*. Genetics 156:1483-92.
767 55. Levin-Reisman I, Fridman O, Balaban NQ. 2014. ScanLag: high-throughput
768 quantification of colony growth and lag time. J Vis Exp doi:10.3791/51456.
769 56. Benaglia T, Chauveau D, Hunter DR, Young DS. 2010. mixtools: An R Package for
770 Analyzing Mixture Models. Journal of Statistical Software 32.
771 57. Wickham HS, Berlin, 2009). 2009. ggplot2: Elegant Graphics for Data Analysis.
772 Springer, Berlin.
773 58. Chiarelli A, Cabanel N, Rosinski-Chupin I, Zongo PD, Naas T, Bonnin RA, Glaser P.
774 2020. Diversity of mucoid to non-mucoid switch among carbapenemase-producing
775 *Klebsiella pneumoniae*. BMC Microbiol 20:325.
776 59. Bankevich A, Nurk S, Antipov D, Gurevich AA, Dvorkin M, Kulikov AS, Lesin VM,
777 Nikolenko SI, Pham S, Prjibelski AD, Pyshkin AV, Sirotkin AV, Vyahhi N, Tesler G,
778 Alekseyev MA, Pevzner PA. 2012. SPAdes: a new genome assembly algorithm and its
779 applications to single-cell sequencing. J Comput Biol 19:455-77.
780 60. Koren S, Walenz BP, Berlin K, Miller JR, Bergman NH, Phillippy AM. 2017. Canu:
781 scalable and accurate long-read assembly via adaptive k-mer weighting and repeat
782 separation. Genome Res 27:722-736.
783 61. Hunt M, Silva ND, Otto TD, Parkhill J, Keane JA, Harris SR. 2015. Circlator:
784 automated circularization of genome assemblies using long sequencing reads. Genome
785 Biol 16:294.
786 62. Deatherage DE, Barrick JE. 2014. Identification of mutations in laboratory-evolved
787 microbes from next-generation sequencing data using breseq. Methods Mol Biol
788 1151:165-88.
789 63. Milne I, Stephen G, Bayer M, Cock PJ, Pritchard L, Cardle L, Shaw PD, Marshall D.
790 2013. Using Tablet for visual exploration of second-generation sequencing data. Brief
791 Bioinform 14:193-202.
792 64. Seemann T. 2014. Prokka: rapid prokaryotic genome annotation. Bioinformatics
793 30:2068-9.
794 65. Wyres KL, Nguyen TNT, Lam MMC, Judd LM, van Vinh Chau N, Dance DAB, Ip M,
795 Karkey A, Ling CL, Miliya T, Newton PN, Lan NPH, Sengduangphachanh A, Turner
796 P, Veeraraghavan B, Vinh PV, Vongsouvath M, Thomson NR, Baker S, Holt KE. 2020.

797 Genomic surveillance for hypervirulence and multi-drug resistance in invasive
798 *Klebsiella pneumonia*e from South and Southeast Asia. Genome Med 12:11.
799 66. Bortolaia V, Kaas RS, Ruppe E, Roberts MC, Schwarz S, Cattoir V, Philippon A,
800 Allesoe RL, Rebelo AR, Florensa AF, Fagelhauer L, Chakraborty T, Neumann B,
801 Werner G, Bender JK, Stingl K, Nguyen M, Coppens J, Xavier BB, Malhotra-Kumar
802 S, Westh H, Pinholt M, Anjum MF, Duggett NA, Kempf I, Nykäsenoja S, Olkkola S,
803 Wieczorek K, Amaro A, Clemente L, Mossong J, Losch S, Ragimbeau C, Lund O,
804 Aarestrup FM. 2020. ResFinder 4.0 for predictions of phenotypes from genotypes. J
805 Antimicrob Chemother doi:10.1093/jac/dkaa345.
806 67. Carattoli A, Zankari E, Garcia-Fernandez A, Voldby Larsen M, Lund O, Villa L, Moller
807 Aarestrup F, Hasman H. 2014. In silico detection and typing of plasmids using
808 PlasmidFinder and plasmid multilocus sequence typing. Antimicrob Agents Chemother
809 58:3895-903.
810 68. Varet H, Brillet-Guéguen L, Coppée JY, Dillies MA. 2016. SARTools: A DESeq2- and
811 EdgeR-Based R Pipeline for Comprehensive Differential Analysis of RNA-Seq Data.
812 PLoS One 11:e0157022.
813 69. Racine JS. 2012. RStudio: A Platform-Independent IDE for R and Sweave. Journal of
814 Applied Econometrics 27:167-172.
815

816

817 **FIGURE LEGENDS**

818

819 **Fig. 1. Diversity of resistance and heteroresistance.** (A) Visualization of the HR profiles by
820 Etest. Three different categories were distinguished (HR, moderate HR and absent HR). Isolates
821 showing full contact with the antibiotic strip (on the right) were excluded from further analyses
822 and classified as "HR not detectable" (Table S1); (**B**) Occurrence of HR among KPC isolates.
823 SIR = Susceptible/Intermediate/Resistant. Bar colors: dark grey = imipenem (IMP), light grey
824 = meropenem (MEM). Yes = presence of HR (including HR and moderate HR isolates), No =
825 absence of HR. Isolates that showed full contact with the antibiotic strip (n = 31 for MEM and
826 n = 3 for IMP) were not included; (**C**) Correlation between HR profile and type of KPC
827 carbapenemase. Bar colors: Blue = KPC-2; Orange = KPC-3; yes for HR and no for non-HR.

828

829 **Fig. 2. Population analysis profiling (PAP) of 13 CPKp clinical isolates (A)** Results were
830 expressed in $\log_{10}$ of the frequency of survival at 4-FOLD, 8-FOLD, 10-FOLD the
831 concentration of IMP relative to the MIC of the isolate as determined by Etest. Isolates names
832 are indicated at the top of each chart. Red bars: KPC isolates; magenta bars: VIM isolates; green
833 bars: NDM isolates; blue bars: OXA isolates. The red dashed line indicates the cutoff value (-
834 5) above which counts were considered significant. (**B**) Impact of the bacterial growth phase on
835 the survival to different doses of imipenem. Green bars indicate plating from exponentially
836 growing cultures, whereas orange indicates plating from stationary phase bacterial cultures.

837 Data were calculated from five independent experiments. Significant results were highlighted:
838 * *p*-value ranging from 0.0159 to 0.0278; ** *p*-value ranging from 0.0025 to 0.093.
839
840 **Fig 3. Heterogeneous survival of KPC-Kp to high concentrations of IMP (A)** Histograms
841 of single-colony time of appearance from exponentially growing cultures. Colony appearance
842 time was monitored every 20 minute over 48-hours incubation on plate. ToA = Time of
843 Appearance; cyan blue bars represent colonies appearing on drug-free media, whereas red bars
844 indicate colonies growing onto IMP-containing agar plates. The data are an overlap of at least
845 three independent replicates per each isolate and each condition. (**B)** Fit of two-mixture
846 component model to the distributions of ToA for each isolates after plating from exponential
847 phase cultures. In red, population 1 (N1), and in blue the population 2 (N2). The representation
848 is an overlap of at least three independent replicates per isolate and per condition. ToA data are
849 expressed as density rather than count. Estimated parameters of each subpopulations and
850 replicates are given in Table S2. Note that, for the isolate BIC-1, the model failed to fit a normal
851 distribution to the tail. (**C)** Comparison of Lag Time Extension (LE) of N1 subpopulations from
852 the six isolates plated from EP and SP cultures. Only significant differences were highlighted
853 (* corresponds to *p*-value = 0.033, ** corresponds to *p*-value = 0.0025). LE was calculated as
854 the mean ToA value of N1 population over the mean ToA value of untreated population. **(D)**
855 Frequency of persisters calculated according to the methodology proposed by Balaban et al
856 (28) from at least three replicates (data are available in Table S2). Colonies appearing after the
857 cutoff value (calculated as ToA > $\mu+3\Sigma$, where μ= estimated ToA mean for N1 and Σ =
858 estimated standard deviations) were defined as persisters. Frequencies were calculated as the
859 proportion of CFU/ml of each subpopulation over the total number of CFU/ml of the initial
860 inoculum. The frequency of persisters was significantly higher in exponential phase rather than
861 in stationary phase for CNR146C9 isolate (**, *p*-value = 0.0038).
862
863 **Fig. 4. Diversity of genetic events detected among colonies from patterns A, B and C. (A)**
864 Diversity of genetic events as identified by using Breseq. **(B)** Functional categories of loci
865 affected by the genetic events as identified in Tables S3, S4 and S5. The three classes of colonies
866 as defined by their ToA and growth rate, A, B and C are indicated in green, red and blue
867 respectively.
868
869 **Fig 5. DNA amplification and pKPC copy numbers in pattern A isolates.** (**A)** Duplication
870 of a 89584 bp region in strain AC376-A. The relative copy number was estimated compared to

871 the parental stain CNR146C9 based on the count of number of reads counted per gene. The
872 duplicated region is in blue and contains as candidate locus contributing to increased IMP MIC
873 the division and cell wall (dcw) locus (in orange). The insertion of the duplicated copy occurred
874 11 bp upstream *ygiW* with a 5 bp (GAGAA) duplication. *ygiW* expression is activated by the
875 two component regulatory system QseBC encoded by two genes in the opposite orientation.
876 Limits of the duplicated region and insertion sites were deduced from chimeric reads as
877 identified by using Breseq (62)**. (B)** Duplication of a c.a. 68 kb region within the pKPC plasmid
878 in strain AC150-A. Average copy number of the 115 CDS of pKPC was calculated relative to
879 the corresponding average value for all isolates except those having lost pKPC. The central part
880 of the duplicated region is highly similar to a pCTX-M-15 DNA regions lost in this strain and
881 explaining the variable and lower copy number as quantified by counting mapping reads (C)
882 Average copy number of pKPC CDSs compared to the average copy number of pKPC CDS
883 across all isolates, except those having lost pKPC. In blue, A isolates; in orange, B isolates and
884 in green, C isolates.
885
886

A

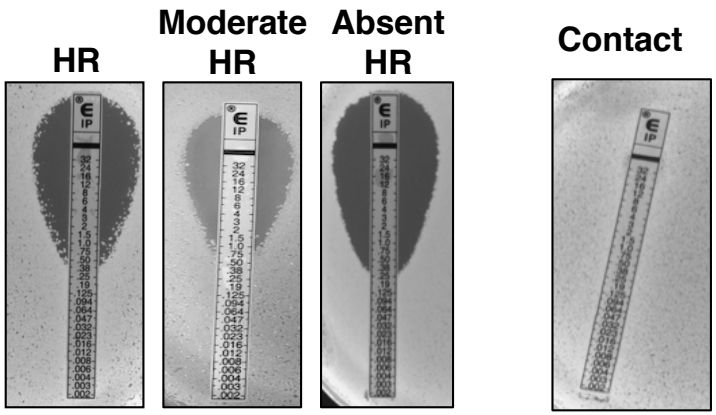
HR
Moderate HR
Absent HR
Contact

B

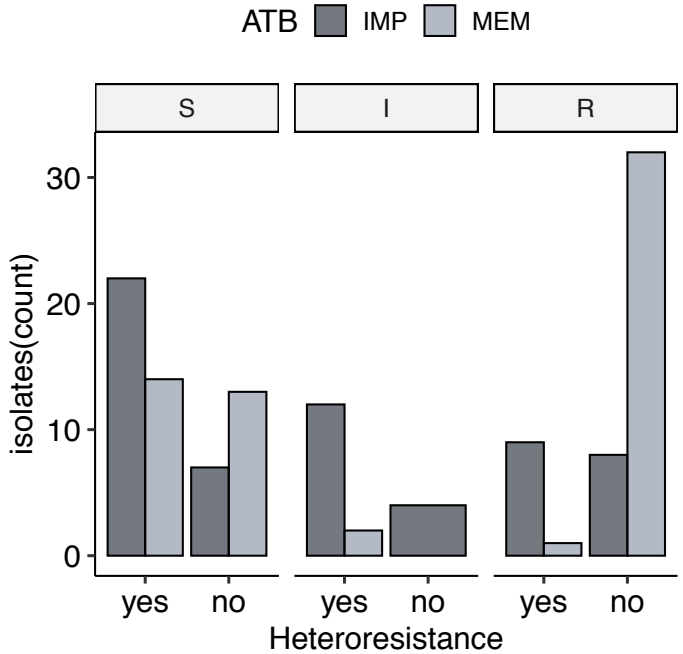
ATB
IMP
MEM
S
I
R
isolates(count)
0
10
20
30
yes
no
yes
no
yes
no
Heteroresistance

C

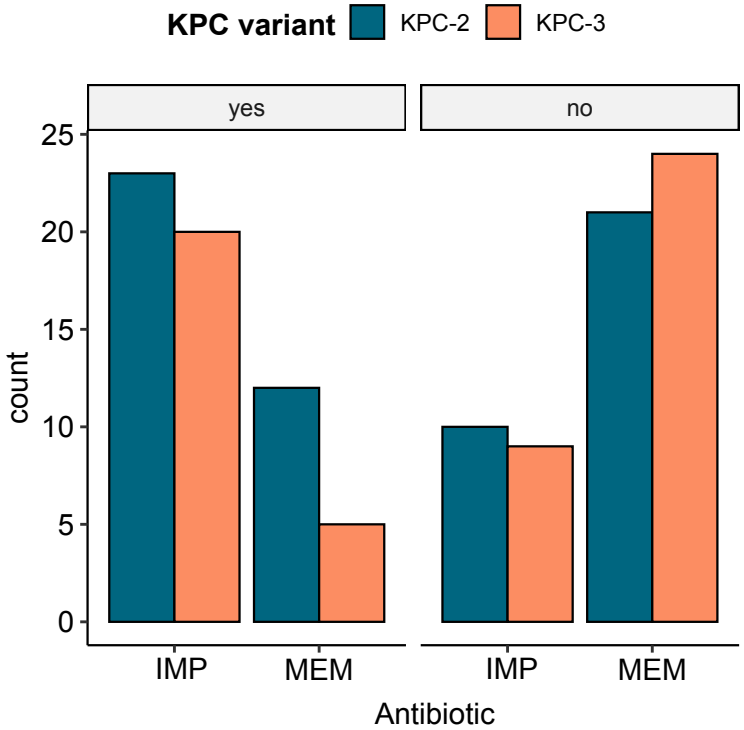
KPC variant
KPC-2
KPC-3
yes
no
count
0
5
10
15
20
25
IMP
MEM
IMP
MEM
Antibiotic

Fig.1

A

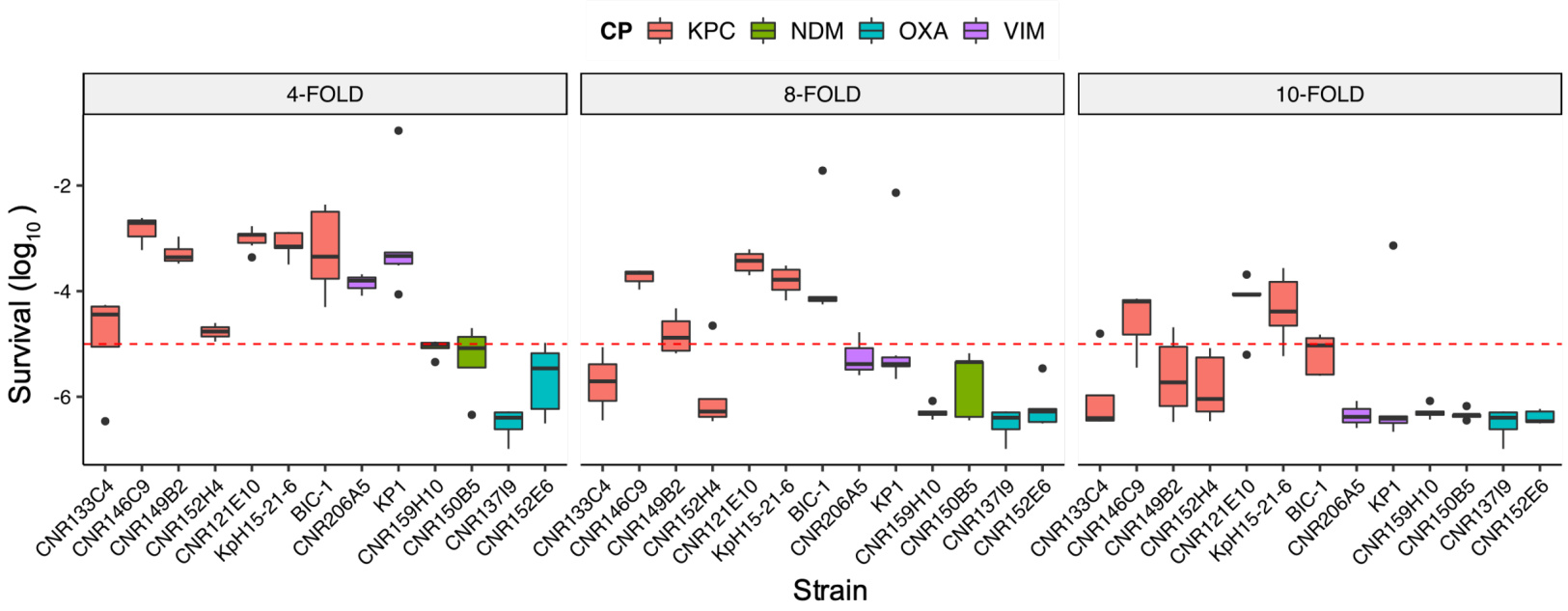
CP KPC NDM OXA VIM
4-FOLD
8-FOLD
10-FOLD
Survival (log10)
-2
-4
-6
CNR133C4
CNR146C9
CNR149B2
CNR152H4
CNR121E10
KpH15-21-6
BIC-1
CNR206A5
KP1
CNR159H10
CNR150B5
CNR137I9
CNR152E6
Strain

B

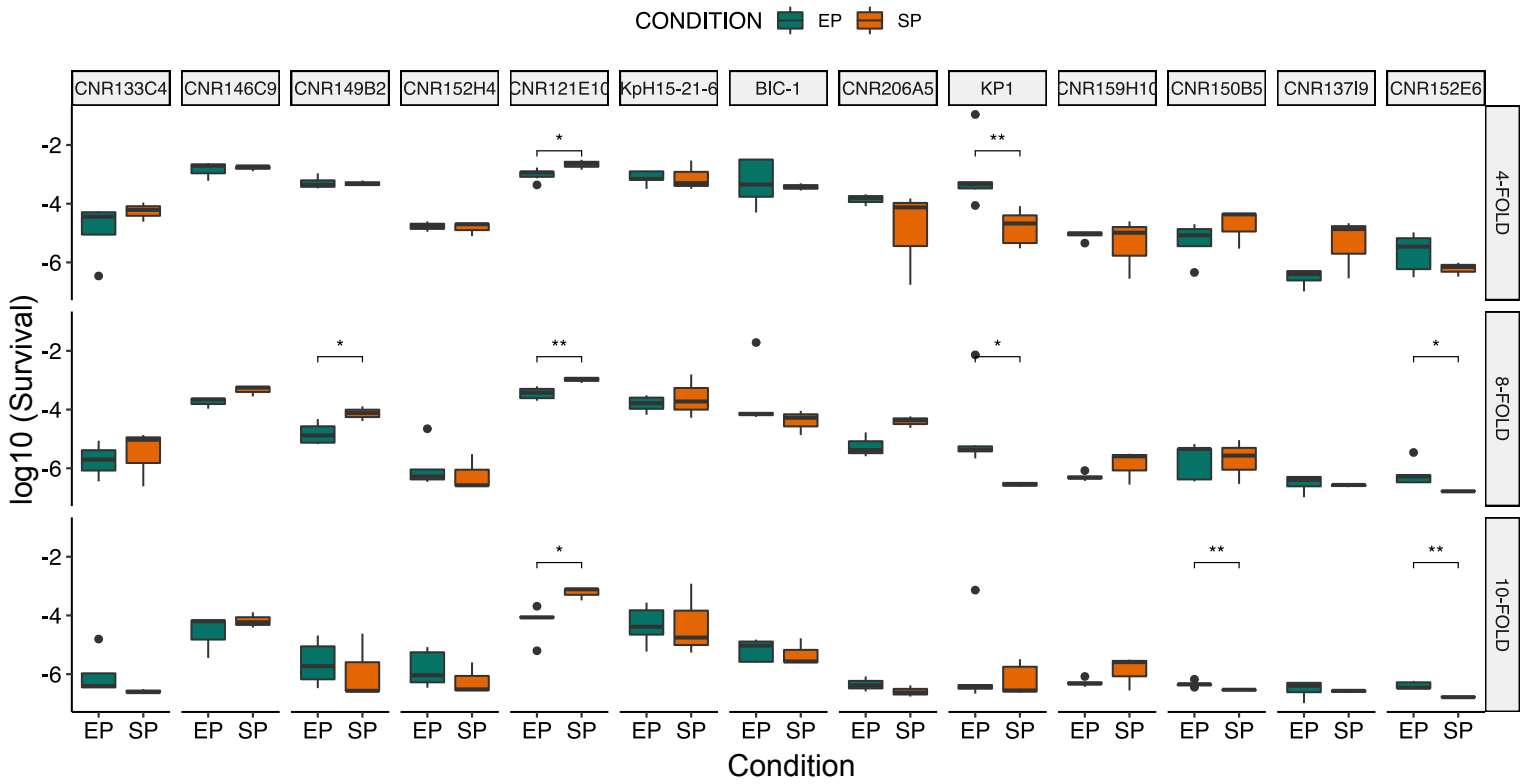
CONDITION EP SP
CNR133C4
CNR146C9
CNR149B2
CNR152H4
CNR121E10
KpH15-21-6
BIC-1
CNR206A5
KP1
CNR159H10
CNR150B5
CNR137I9
CNR152E6
4-FOLD
8-FOLD
10-FOLD
log10 (Survival)
-2
-4
-6
EP SP
Condition

Fig.2

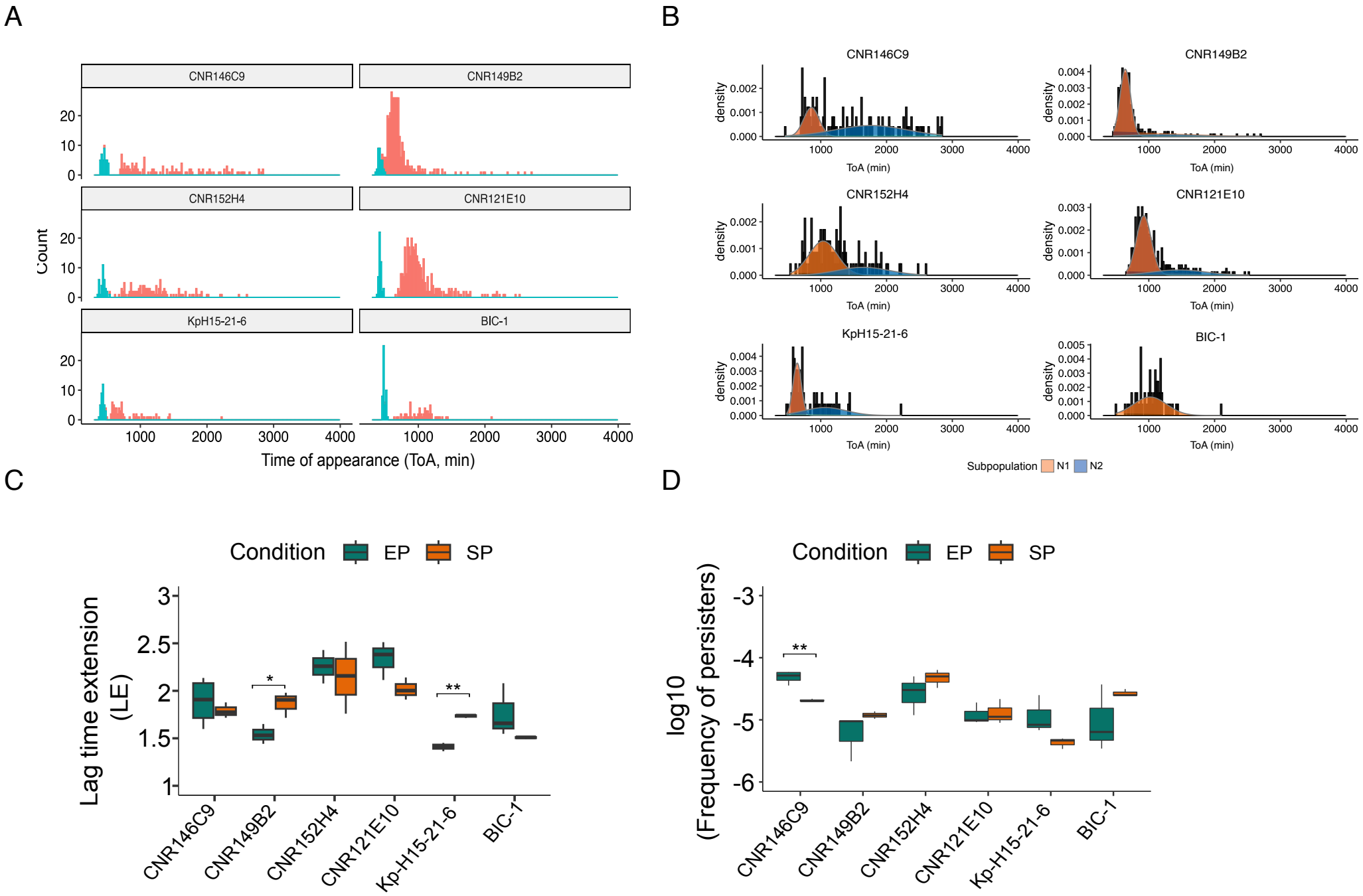
A
CNR146C9
CNR149B2
CNR152H4
CNR121E10
KpH15-21-6
BIC-1
Count
Time of appearance (ToA, min)
B
density
ToA (min)
Subpopulation N1 N2
C
Condition EP SP
Lag time extension (LE)
D
log10 (Frequency of persisters)

Fig.3

A

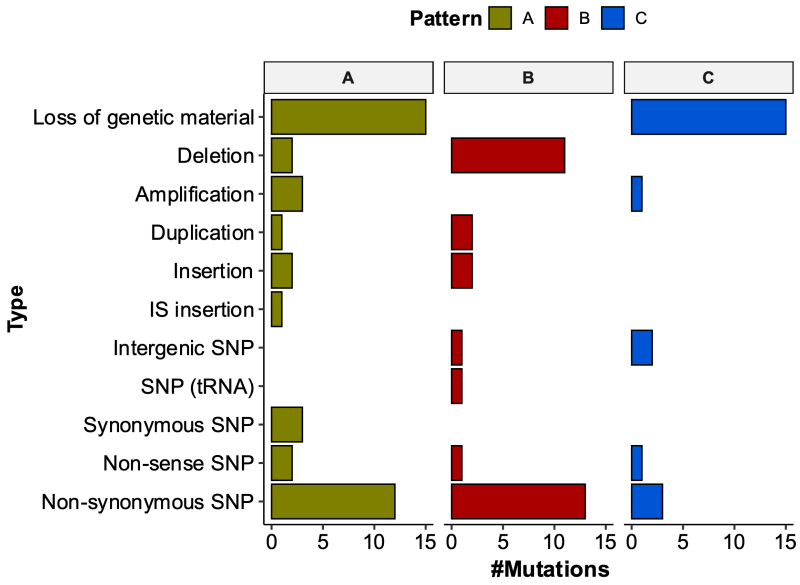
Pattern A B C
A
B
C
Loss of genetic material
Deletion
Amplification
Duplication
Insertion
IS insertion
Intergenic SNP
SNP (tRNA)
Synonymous SNP
Non-sense SNP
Non-synonymous SNP
Type
0 5 10 15
#Mutations

B

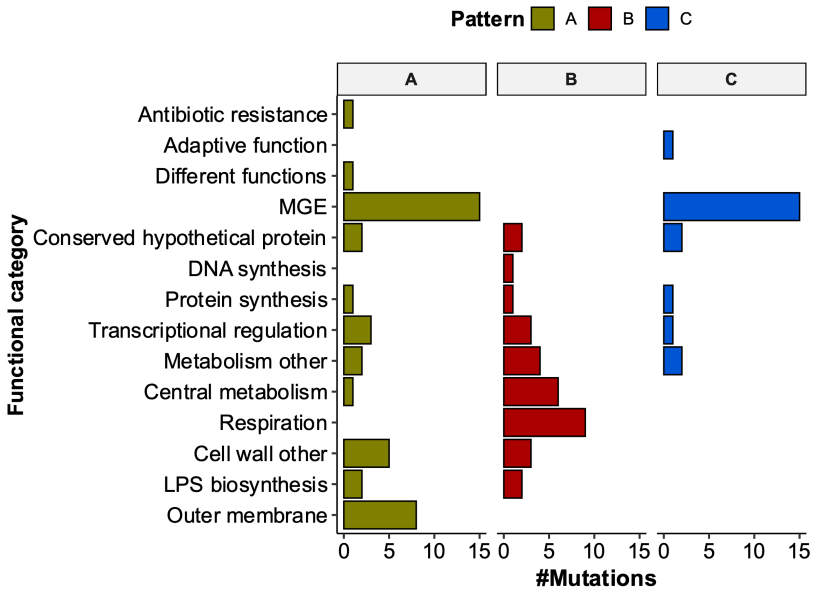
Pattern A B C
A
B
C
Antibiotic resistance
Adaptive function
Different functions
MGE
Conserved hypothetical protein
DNA synthesis
Protein synthesis
Transcriptional regulation
Metabolism other
Central metabolism
Respiration
Cell wall other
LPS biosynthesis
Outer membrane
Functional category
0 5 10 15
#Mutations

Fig.4

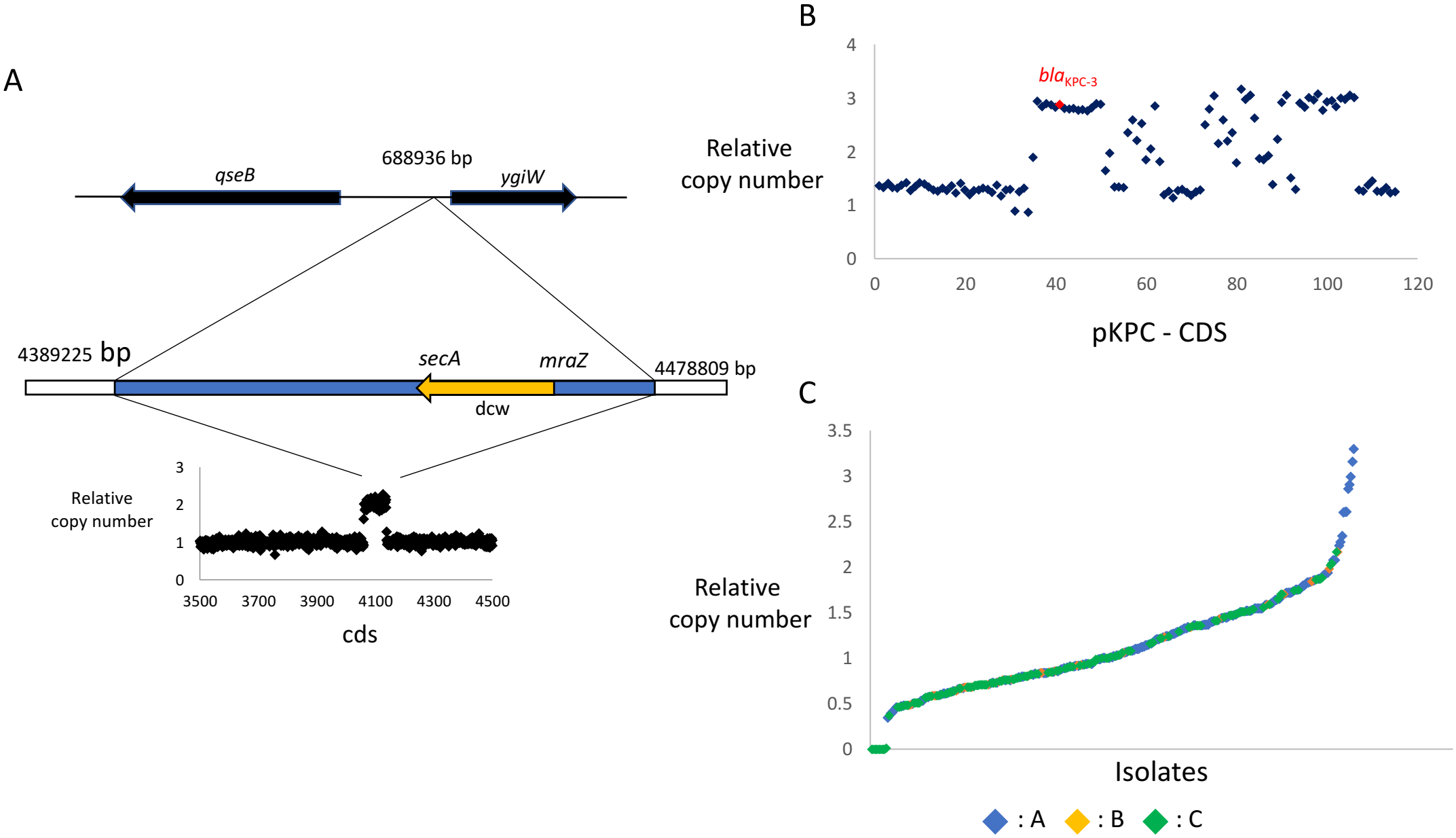
A
688936 bp
qseB
ygiW
4389225 bp
secA
mraZ
4478809 bp
dcw
Relative
copy number
3
2
1
0
3500
3700
3900
4100
4300
4500
cds
B
Relative
copy number
blaKPC-3
4
3
2
1
0
0
20
40
60
80
100
120
pKPC - CDS
C
Relative
copy number
3.5
3
2.5
2
1.5
1
0.5
0
Isolates
: A
: B
: C

Fig.5

A.

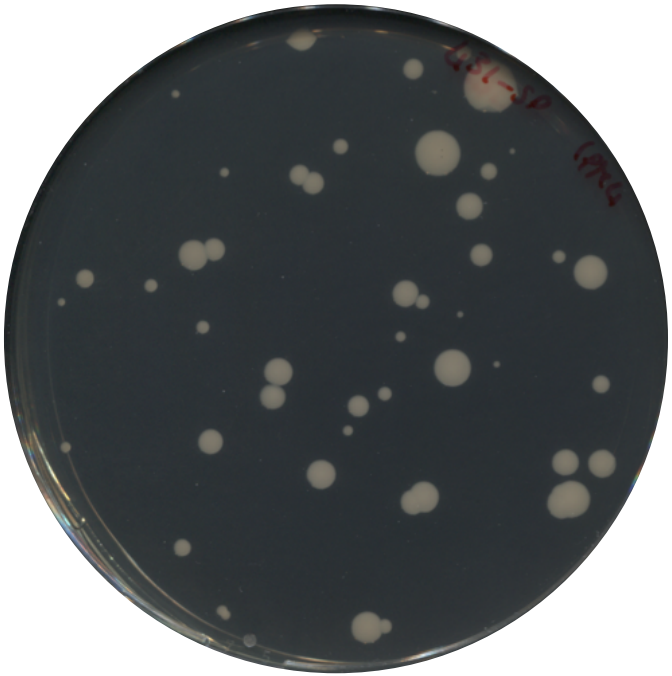

B.

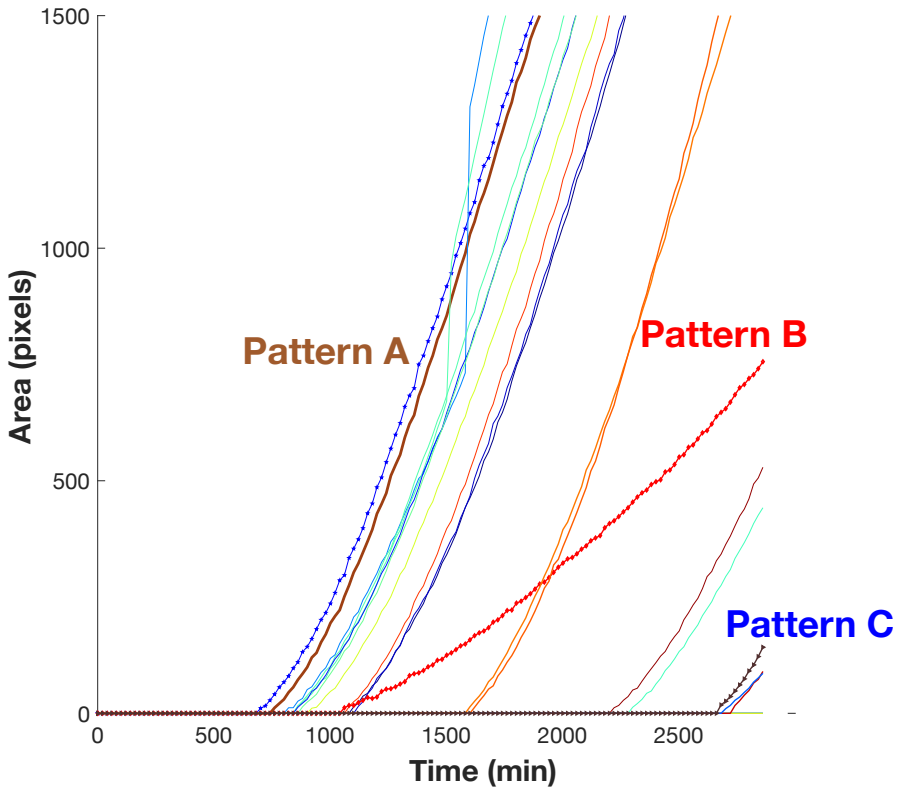

Fig. S1 Heterogeneity of colony growth as detected by ScanLag. (A) Example of plate containing colonies from the isolate CNR146C9 emerging on media supplemented with imipenem at 8-fold the MIC as determined by Etest. Colonies exhibit heterogeneous size and morphology, reflected by different Time of Appearance and Growth rates. **(B)** Colony growth curves as determined by ScanLag. Three patterns (A, B and C) were described according to the time of appearance and the growth rate.

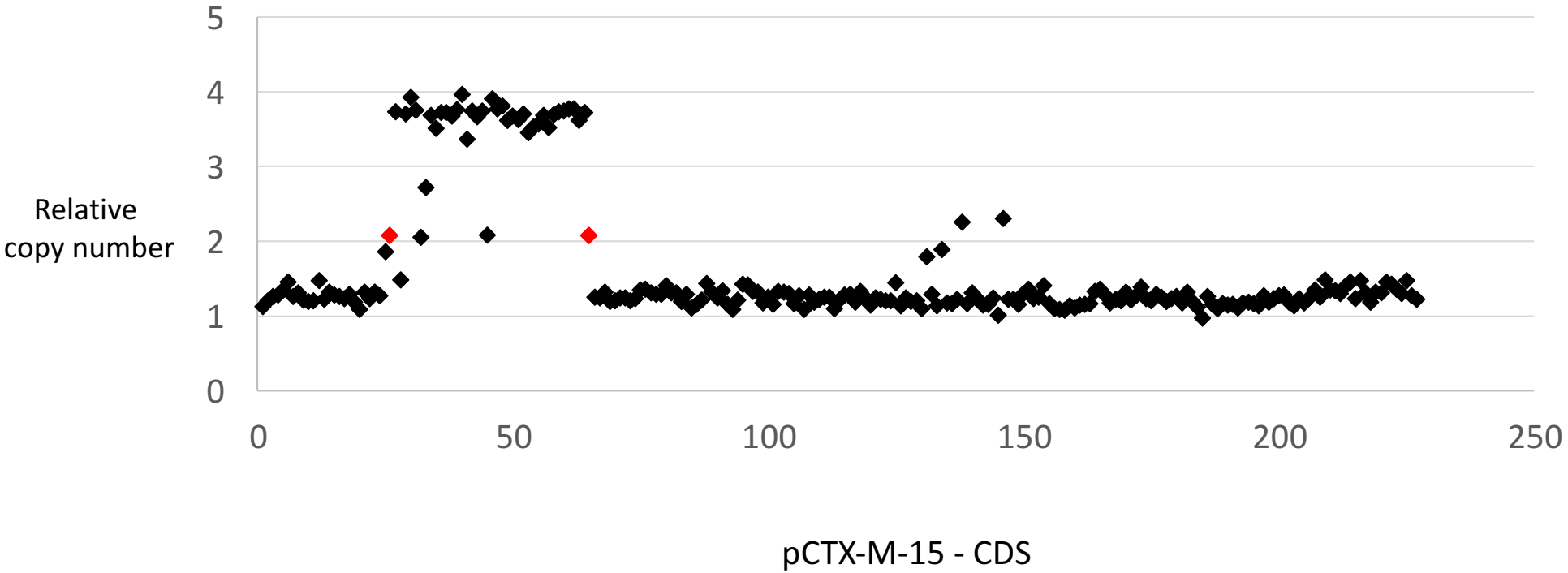

Fig. S2 DNA amplification in pCTX-M-15. Duplication of a c.a. 49 kb region within the pCTX-M-15 plasmid in strain AC362-C. Average copy number of the 227 CDS of pCTX-M-15 was calculated relative to the corresponding average value for all isolates. Genes are indicated by diamonds; in red, the two IS*5075* bracketing the duplication.